# Rectified motion in an asymmetric channel: The role of hydrodynamic interactions with walls

Behzad Golshaei[1] and Ali Najafi[2,*]

[1]*Department of Physics, Institute for Advanced Studies in Basic Sciences (IASBS), Zanjan 45137-66731, Iran*

[2]*Physics Department, University of Zanjan, Zanjan 45371-38791, Iran*

(Received 28 September 2014; revised manuscript received 24 December 2014; published 2 February 2015)

Dynamics of a Brownian particle in an asymmetric microchannel that is subjected to an external oscillating force is numerically analyzed. In addition to the elastic collisions with the walls that are kind of short range interactions, the long range hydrodynamic influences of the walls have been considered in an approximate way. We demonstrate how the geometrical parameters of the channel change the rectified current of the particle. As a result of numerical calculations, we show that long range hydrodynamic interactions with walls decrease the efficiency of the Brownian ratchet.

DOI: 10.1103/PhysRevE.91.022101 PACS number(s): 05.40.−a, 05.60.−k, 47.15.G−

## I. INTRODUCTION

For a Brownian particle that is in thermal equilibrium, second low of thermodynamics does not allow us to achieve a rectified motion even when the particle is moving in an asymmetric periodic potential. In addition to symmetry breaking with an externally applied asymmetric periodic potential, the fluctuations need to obey an out of equilibrium statistics to achieve a rectified motion at the microscopic world. The original idea of the rectification of random motions at microscopic scales dates back to the work by Smoluchovski [1] where he discussed the issue of extracting useful work from fluctuations. Feynman has illustrated this idea by a very intuitive gedanken experiment composed of ratchet and pawl [2]. Very recently, a group of experimentalists have shown how the ratchet idea can be tested at macroscopic world by using a granular gas. In their experiment, a plate vibrating vertically provides a nonequilibrium gas of granular particles. Collision of these granular particles with four vanes of an asymmetric rotary part enforce it to rotate. The overall motion of the vanes is shown to be a rectified rotation in a direction preferred by the asymmetry of the vanes [3].

In addition to the above fundamental interests on the physics of Brownian ratchet, it also provides a basic physical mechanism for describing the dynamics of most biophysical molecular motors [4]. Transport of colloidal particles in channels with the size of micrometer is another related area. Recent technological advances allow researchers to design and fabricate devices to guide particles on micro- and nanochannels [5,6]. Flow control and separation of particles in such channels are the main experimental interests in this field [7,8]. An important category of microfluidic devices is so-called rocked ratchet, where an applied oscillating force drives a net drift velocity for particles fluctuating in an asymmetric potential imposed by the walls of channel. The physical mechanism behind such systems has been considered in detail [9,10]. A very comprehensive review of the related works is presented in an article by Hanggi [11]. Hydrodynamic interaction between particles at intermediate and high volume fraction of particles is proved to have prominent effects on the efficiency of Brownian ratchets [12]. In addition to interaction between particles, the long range hydrodynamic interaction with confining walls is proved to have essential effects on the motion of either passive colloidal particles [13,14] or active systems [15–17]. It is the main goal of this article to address how the interaction with walls will influence the functionality of a Brownian ratchet. Usually this kind of long range interaction is neglected in theoretical and numerical investigations [18]. In this paper, we focus on hydrodynamic interactions of particles with the walls of channel. To answer this question, we start by a perturbation based theory that can give estimated values of the hydrodynamic interactions for a spherical particle moving near confining walls. Then allowing the particle to fluctuate, we numerically simulate the Brownian dynamics of such a colloidal particle moving in a medium confined with the walls of an asymmetric channel.

The structure of this article is as follows: In Sec. II, we define the model and present the details of approximations for the hydrodynamic interactions. In Sec. III, we present the details of numerical scheme that we have used to simulate the Brownian dynamics. The results are presented in Sec. IV, and finally we discuss in Sec. V.

## II. MODEL AND ITS PARAMETERS

A two dimensional rocked ratchet channel is used to study the transport of Brownian particles. As depicted in Fig. 1, the channel is characterized by its periodic length $L_x$, input and output opening sizes $L_z$, and asymmetry angle $\theta$. For $\theta = 0$, the channel is symmetric and we do not expect any rectified motion for this case. Moreover we assume that the colloidal particle has mass $m$ and its radius is given by $a$. In a reference frame that is shown in the figure, the position vector of the particle is given by $\mathbf{r} = (x,z)$, where $\hat{\mathbf{x}}$ points along the axis of channel. The following stochastic Langevin differential equation describes the dynamics of a colloidal particle moving in this channel [19]:

$$m\ddot{\mathbf{r}} = -\mathbf{G}\cdot\dot{\mathbf{r}} + \mathbf{F}_{hc} + \mathbf{F}_e(t) + \Gamma(t), \tag{1}$$

where $\mathbf{G}$ stands for the hydrodynamic friction tensor and $\Gamma(t)$ shows the random forces due to thermal fluctuations. The effects of the walls of channel are given by a hard core force $\mathbf{F}_{hc}$. As a result of this very short range potential, the dynamics of the particle obeys the rules of elastic collision

*najafi@znu.ac.ir

 

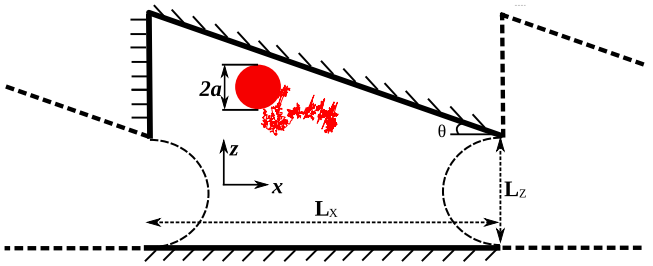


FIG. 1. (Color online) A Brownian particle with radius $a$ moves in a two dimensional rocked Ratchet microchannel with period $L_x$. The input and out of the channel have same width given by $L_z$. Angle $\theta$ measures the asymmetry of channel. A typical trajectory of the Brownian particle moving near the wall is shown.

at the boundaries. Conservation of energy and momentum provide relations for the state of the system before and after each collision. To provide an out of equilibrium condition for the particle, we apply an external force along the $\hat{\mathbf{x}}$ direction that is spatially uniform but period in time:

$$\mathbf{F}_e(t) = f_0 \sin(\omega t)\hat{\mathbf{x}}, \tag{2}$$

where $f_0$ and $\omega$ show the amplitude and frequency of the external force, respectively. In addition to the above deterministic forces, the dynamics of the particle is influenced by time dependent random noise $\Gamma(t)$ resulting from thermal fluctuations. The average and correlation of this stochastic force is given by

$$\langle \Gamma(t) \rangle = 0, \quad \langle \Gamma(t)\Gamma(t') \rangle = 2k_B T \mathbf{G} \delta(t - t'), \tag{3}$$

where $k_B T$ is the thermal energy.

What we are interested in this article is the effects of long range hydrodynamic interaction with the walls of the channel. All of the information related to the hydrodynamic interactions with the walls are encoded in the friction tensor $\mathbf{G}$. In addition to the size of colloid, this friction tensor depends on the distance between the particle and the walls. This friction coefficient, should in principle be derived from solution to Stokes equation, the equation that governs the dynamics of fluid at the scale of micrometer. The solution to this equation, provided that the fluid motion obeys the no-slip boundary conditions on the walls, will reveal the detailed form of the friction tensor. As there is no exact solution to the Stokes equation in an asymmetric channel, we will use approximate prescriptions for the friction coefficients.

Before considering the complicated geometry of our channel, we start by presenting the results for friction coefficients of a particle moving in a semi infinite fluid environment that is bounded by a single wall. Instead of friction tensor, it is more convenient to work with the mobility tensor $\mathbf{M}$ that is the inverse of friction tensor when expressed in the matrix notation: $\mathbf{M} = \mathbf{G}^{-1}$. Figure 2(a), shows a spherical particle with size $a$ immersed in a semi-infinite fluid that has a distance $h$ from a wall. Theoretical analysis based on perturbation theory can give a series expansion for the mobility tensor in terms of small parameter $(a/h)$. In the matrix notation, the

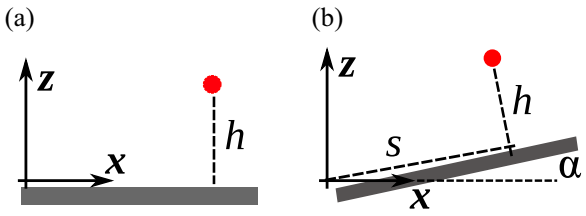


FIG. 2. (Color online) Left: A spherical particle with size $a$ located in a position with a distance $h$ above a flat wall. Right: Same problem, but seen in a frame of reference rotated with an angle $\alpha$ with respect to the wall.

mobility tensor has the following components:

$$\mathbf{M} = \begin{pmatrix} M_{xx} & M_{xz} \\ M_{zx} & M_{zz} \end{pmatrix}. \tag{4}$$

Symmetry considerations do not allow nonzero off-diagonal elements for the mobility tensor: $M_{xz} = M_{zx} = 0$, and the other components are given by [14,20]

$$M_{xx} = \mu \left[ 1 - \frac{9}{16}\left(\frac{a}{h}\right) + \frac{1}{8}\left(\frac{a}{h}\right)^3 - \frac{1}{16}\left(\frac{a}{h}\right)^5 + \mathcal{O}\left(\frac{a}{h}\right)^7 \right],$$
$$M_{zz} = \mu \left[ 1 - \frac{9}{8}\left(\frac{a}{h}\right) + \frac{1}{2}\left(\frac{a}{h}\right)^3 - \frac{1}{8}\left(\frac{a}{h}\right)^5 + \mathcal{O}\left(\frac{a}{h}\right)^7 \right],$$

where $\mu = 1/(6\pi\eta a)$, is the self-mobility of a spherical particle with size $a$ moving in a fluid with viscosity $\eta$. Using the above components for the mobility tensor, one can write a perturbation series for the friction tensor as

$$\mathbf{G} = \mathbf{G}_0 + \delta\mathbf{G}, \tag{5}$$

where $\mathbf{G}_0 = 6\pi\eta a\mathbf{I}$ is the friction tensor for a sphere moving in an infinite fluid and $\mathbf{I}$ is the unit tensor (unit matrix in matrix representation). Here all of the corrections due to the presence of wall are collected in $\delta\mathbf{G}$. Direct calculations can give the explicit mathematical form of this correction term.

Figure 2(b) shows the same problem as above, but in a reference frame that is rotated with an angle $\alpha$ with respect to the wall. It is a straightforward geometrical calculation to express the mobility tensor in the rotated frame. In terms of the mobility tensor in the plate frame (frame in which the axis are parallel and perpendicular to the wall), the mobility tensor in the rotated frame can be given by

$$\mathbf{M} = \mathcal{R}^T(\alpha) \cdot \mathbf{M} \cdot \mathcal{R}(\alpha), \tag{6}$$

where the dot symbol represents the matrix multiplication rule and $\mathcal{R}(\alpha)$ is the rotation matrix with an angle $\alpha$ about axis $\hat{\mathbf{x}} \times \hat{\mathbf{z}}$.

How will a particle moving in a medium confined within the walls of a complicated channel respond to an external force? Exact solutions to this question occur only in a certain type of symmetric geometries. A cylindrical channel with infinite length and also a rectangular channel with infinite length and infinite depth are examples with exact solutions [21]. Apart from the above symmetric geometries, there is no analytic solution for the hydrodynamic friction problem in an asymmetric channel. Among different approximate methods, the direct superposition of the corrections from different walls is the simplest approximate scheme that can give the effects of

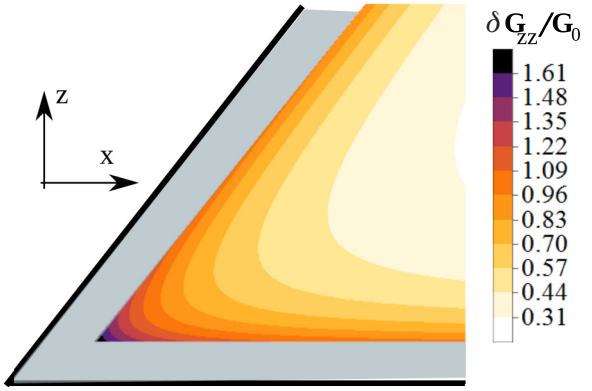


FIG. 3. (Color online) $\delta G_{zz}$ is plotted inside a $\pi/4$ rad corner. The gray region near the walls represents the geometrically inaccessible part for a rigid sphere with radius $a$. The effects due to the walls decay for regions very far from the walls.

walls in a channel [22,23]. For a particle moving in a channel with confining walls, the friction tensor may be written as

$$\mathbf{G} = \mathbf{G}_0 + \sum_i \delta\mathbf{G}^i, \tag{7}$$

where $\delta\mathbf{G}^i$ is the correction due to the $i$th wall of the channel. Using this approximation we can study the dynamics of a Brownian particle moving in the channel.

To have a feeling of the correction to the friction coefficient due to the presence of walls, we have plotted in Fig. 3 one of the components of $\delta G$ in a corner constructed by two intersecting walls. As the sphere has a finite radius, only a part of the corner is accessible to the sphere. The value of the correction function $\delta G$ is plotted for the accessible region. As one can see, this function is finite and large near the walls and it decays to zero far from the walls. Beyond the walls, the friction coefficient decays to its bare value $G_0$ and hence $\delta G$ goes to zero.

Now for a unit cell in our channel, three walls confine the fluid. Here the friction coefficient will have contributions that come from these three walls. Considering the results of Fig. 3, we are sure that in the middle of the channel (midregion of each cell) the effects of walls decay to zero and the friction coefficient will reach its bare value $G_0$.

At the entries of the channel and using the above prescription, the vertical and tilted walls will have great contributions that are nonphysical. We should exclude these nonphysical contributions. As it is shown in Fig. 1, we have turned off the hydrodynamic interactions for the regions in the entries of channel. These two regions, where the interactions are turned off, are shown by dotted lines (semicircles) at the entries. A particle feels the hydrodynamic interactions when it crosses this dotted lines. This trick allow us to exclude the effects of nonphysical parts of the vertical and tilted boundaries. A Brownian particle crossing these dotted lines will feel a discontinuity in the friction coefficient. We will argue later that such a discontinuity does not have a crucial influence on our results.

The validity of the superposition method that is used here is a challenging issue and it will break near the walls and especially at the corners. At distances very near to the wall, the short range hard core interaction dominates the dynamics of the particle and we do not expect to see any sharp effect from the breakdown of our approximation for hydrodynamic interactions. Second, because of the geometrical constraints, we will see that the particle does not allow us to reach the corners at all. These will ensure that the superposition approximation will correctly account for the long range hydrodynamic interactions with the wall of channel and we expect to have a picture that is at least qualitatively correct.

## III. NUMERICAL SIMULATION

We define the current density as the number of particles per unit length of the opening that exit from the left side of the channel in a unit time. The density of current for the particles is a quantity that reflects how the motion of particles is rectified. In terms of the average velocity of the particles, we can write the current density as

$$J = n\langle v_x\rangle, \tag{8}$$

where $n$ is the density of particles, the number of particles per unit area in our two dimensional problem. As we are not interested about the hydrodynamic interactions between the particles, we put a single particle in our channel and study its dynamics. For this case the density is given by $n = [L_x L_z(1 + \frac{1}{2}\Delta\tan\theta)]^{-1}$, with $\Delta = L_x/L_z$. Averaging over $\mathcal{N}$ realizations of the system, we can obtain the average velocity as

$$\langle v_x\rangle = \frac{1}{\mathcal{N}}\sum_{i=1}^{\mathcal{N}} \frac{x_i(t_s) - x_i(0)}{t_s}, \tag{9}$$

where $t_s$ is the time of observation (simulation time).

To numerically solve the Langevin differential equation [Eq. (1)], we need to make it nondimensional. For this purpose we can use $a$ as a scale for length and $\tau = a^2/(\mu k_B T)$ as a scale for time and make all variables nondimensional. After going to the dimensionless system of units, all of the dynamical equations can be written in terms of dimensionless variables. Denoting the nondimensional variables with an overbar, the nondimensional overdamped Langevin equation reads

$$\bar{\mathbf{G}}\cdot\bar{\mathbf{r}}' = \bar{f}_0\sin(\bar{\omega}\bar{t}\,)\hat{x} + \bar{\Gamma}, \tag{10}$$

where the prime symbol denotes the derivative with respect to nondimensional time. One should note that the dimensionless Reynolds number $\mathrm{Re} = m\mu/\tau$, which measures the relative importance of acceleration term with respect to the dissipation forces, is very small, $Re = 10^{-3}$, for colloidal particles. For this reason we concentrate on the overdamped equation. The nondimensional amplitude of the external force is given by $\bar{f}_0 = (\mu\tau/a)f_0$ and $\bar{\mathbf{G}} = \mu\mathbf{G}$. The noise satisfies the following correlation function:

$$\langle\bar{\Gamma}(\bar{t})\bar{\Gamma}(\bar{t}')\rangle = 2\bar{\mathbf{G}}\delta(\bar{t} - \bar{t}'). \tag{11}$$

The nondimensional current density can be written as $\bar{J} = J/J_0$, where $J_0 = [\tau L_z(1 + \frac{1}{2}\Delta\tan\theta)]^{-1}$. To calculate the current density and average over realizations, we can use the periodic boundary condition and extract the average value of the current from a long time dynamics of a single particle. Please note that choosing the above sort of nondimensional

system allows us to write the average current density as

$$\bar{J} = \frac{N_R - N_L}{N}, \tag{12}$$

where $N_R$ is the number of times that the particle exits from the right opening and $N_L$ is the number of times that the particle enters the channel from the left side. Here $N = t_s/\tau$ and $t_s$ stands for the simulation time.

We use the method of Ref. [24] to numerically integrate the overdamped equations of motion. To generate random numbers, we use the Mersenne Twister pseudorandom number generator.

Numerical parameters that define our system are as follows: we choose a spherical particle with size $a = 1\ \mu$m moving in a channel that is filled with water and it is at room temperature. The viscosity of water is $\eta = 10^{-3}$ Pa sec and the thermal energy is $k_B T = 0.02$ eV. These will result in a characteristic time scale that is $\tau = 10$ sec. We choose a time step $\Delta t = 0.005$ sec that in dimensionless units is about $\Delta\bar{t} = 0.0005$. Diffusion times along the axis of the channel and along a direction that is perpendicular to its axis are defined by $\tau_D^x = (L_x/a)^2\tau$ and $\tau_D^z = (L_z/a)^2\tau$ respectively. In a channel with typical length $L_x = 15a$, we will see that $\tau_D^x = 2000$ sec. In the following section we will present the results of numerical calculations.

## IV. RESULTS

Before investigating the hydrodynamic effects of the walls, we first turn off the hydrodynamic interaction and consider only the elastic collisions with the walls. To illustrate the functionality of the Brownian ratchet, we have plotted the average current density as a function of frequency of the external force in Fig. 4 (left). The results have been shown for two cases where the random noise is turned on or turned off. The simulation time is $t_s = 5000$ sec. One should note that, for this small simulation time that we have chosen here, only the results at very large frequencies are acceptable. To obtain true physical results, we should keep in mind that the simulation time should be large in a way that $\bar{t}_s\bar{\omega} \gg 1$. As we expect, the existence of thermal noise is essential for the functionality of the Brownian ratchet. In the absence of thermal noise, no rectification is expected. This is evident in the results, where the current at very large frequencies (the acceptable results) disappears for the case where thermal noise is absent. Here the diffusion time along the axis of the channel is about $\tau_D^x = 15^2\tau \sim 2000$ sec and the period of external force for a special point on the graph with $\bar{\omega} = 1$ is given by $T = 2\pi/\omega = (2\pi/1) \times \tau \sim 60$ sec. The value of current at this frequency is $\bar{J} = 2$ which corresponds to a current of particles that is about $J = 2 \times J_0 \sim 10^5$ m$^{-1}$ sec$^{-1}$. Here $t_s/\tau_D^x = 2.5$, but as a result of external force, the particle has a greater chance to travel many times along the axes of the channel. This would result in an overall finite value for both $N_R$ and $N_L$.

In Fig. 4 (right), we have studied the system that is subjected to thermal noise, and investigated its response by changing both the simulation time and frequency of external force. As one can see, by increasing the time of simulation, the height of all nonzero frequency peaks decreases. Increasing the simulations time will result in a smoother behavior for the current at large frequencies. Learning from the results of these graphs, we choose a proper simulation time and investigate the other physical properties of the Brownian ratchet in the following part.

In Fig. 5, we study how the hydrodynamic interactions with the walls will modify the functionality of a Brownian ratchet. We have plotted the current density in terms of both amplitude of the externally applied force and also the asymmetry angle $\theta$. As one can see, in both cases the inclusion of long range hydrodynamic interactions with the walls will significantly decrease the average current density. In terms of the amplitude of external harmonic force, the hydrodynamic interactions with the wall have more influences at large amplitudes. It is interesting that for a Brownian ratchet working at its efficient angle, the long range hydrodynamic interactions will deeply decrease the current.

This current reduction as a result of hydrodynamic interactions may be understood in terms of the friction coefficients. As we have pointed out in Sec. II, for a particle moving near a single wall, the friction coefficient will be increased with a factor proportional to $(a/h)$. This means that for two particles, one moving in an infinite medium and the other moving near

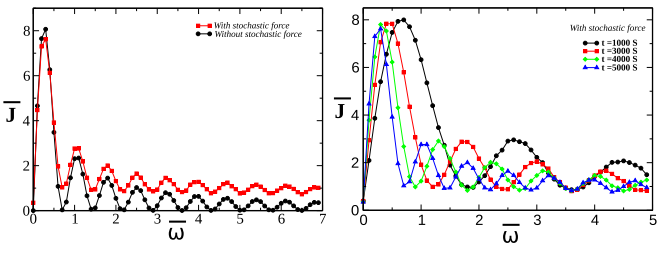


FIG. 4. (Color online) Dimensionless current density is plotted as a function of frequency of external force. Left: simulations have been performed for two cases where thermal force is present or absent. Simulation time is $t_s = 5000$ sec and for different simulation times is plotted. Right: in the absence of thermal noise, the results are shown for different simulation times. In all graphs $\bar{f}_0 = 10$ and the geometrical variables are $a = 1\ \mu$m, $L_x = 15a$, $L_z = 5a$.

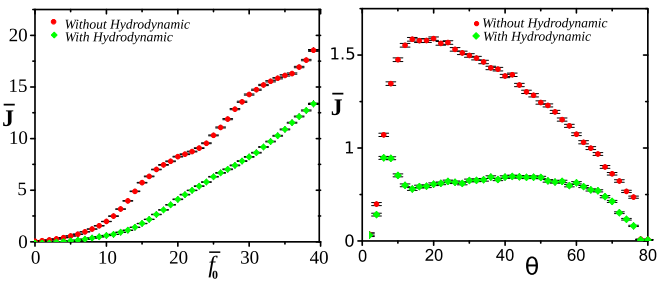


FIG. 5. (Color online) Left: dimensionless current density as a function of the amplitude of external force is plotted for two cases where the hydrodynamic long range interactions with the walls are absent or present. Right: dimensionless current density as a function of the asymmetry angle $\theta$ is plotted for two cases where the hydrodynamic long range interactions with the walls are absent or present. Simulation time is $t_s = 10\,000$ sec, $\bar{f}_0 = 10$, $\bar{\omega} = 100$, $L_x = 15a$, $L_z = 5a$, and $a = 1\ \mu$m.

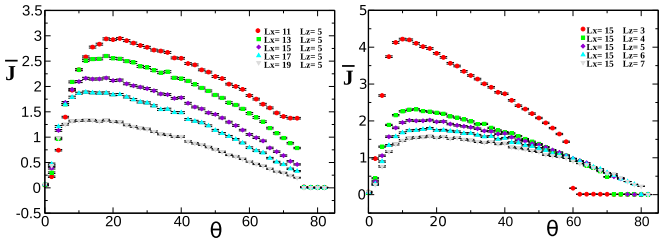


FIG. 6. (Color online) Dimensionless current density as a function of the asymmetry angle $\theta$ for different values of $L_x$ and $L_z$ is investigated. Simulation time is $t_s = 10\,000$ sec, $\bar{\omega} = 100$, and $a = 1\ \mu$m.

a wall, to achieve a constant velocity for both particles, higher force should be applied to the particle that is moving near wall. As the fluctuations are the source of rectified motion here, the increase in the friction coefficient will result in a reduction in the current. This simplified picture that is inspired by a single wall confinement can be applied qualitatively for a particle moving in a complex geometry of a channel.

How do the geometrical parameters of this asymmetric channel influence the functionality of Brownian ratchet? In Fig. 6, we have investigated the influence of geometrical parameters of the system in current density by changing both $L_x$ and $L_z$. The current density is plotted in terms of the asymmetry angle $\theta$. We see that, for fixed $L_x(L_z)$, higher current density can be achieved by choosing smaller $L_z(L_x)$. In all cases, the maximum current density corresponds to an angle $\theta \approx 20^\circ$. Interplay between the size of the particle and the available area in the corners determines the overall behavior of the system. The trapping time for the particle that is moving in the corners of the channel will change the efficiency of a Brownian ratchet. Dividing the area of the channel into two parts, one with a rectangular geometry with an area $L_x \times L_z$ and the second part with a triangle area, we see that less area for the rectangular part corresponds to more current density.

As we pointed out before, when a particle crosses the boundaries where the hydrodynamic interactions are turned off (dotted line in Fig. 1), a discontinuity in the friction coefficient will happen. This can be treated as a discontinuity in friction force. To estimate the order of this force one can assume that in the worse case, the friction drop has a value of about $6\pi\eta a$. For our micron size Brownian particle moving with velocity about 1 $\mu$m/sec, one can reach a force of about $10^{-14}N$. This is comparable with the thermal noise given by $\sqrt{6\pi\eta a k_B T/\Delta t}$. This shows that such discontinuity can be considered as an extra noise in the boundaries. For a typical simulation, this extra noise appears only in 0.01% of all time steps. This shows that such rare events are not able to change the statistics of noise and hence they do not influence our results.

The validity of the superposition approximation can be understood in terms of the back flow method described in Ref. [22]. Flow generated from a moving object propagates and reaches the boundaries. To satisfy the no-slip boundary condition on the walls, a back flow will be produced on the walls as well. A scattered back flow due to a certain wall reaches the other walls and to ensure the satisfaction of boundary conditions on these walls, we need to add second order scattered back flow. This will result in a hierarchy of scattered flows from different walls. Combining all the scattered back flows will modify the motion of a moving object inside the confined flow. Due to the fact that flow from a point force decays like $1/r$, the $N$th order of scattered flow is at least smaller with a factor like $a/h$ with respect to $(N-1)$th order, in the region far from all walls. Simple superposition of the effects due to different walls is an approximation that is achieved by cutting the hierarchy of scattered back flows at its first order. However one should note that the superposition approximation will give an estimation for the real values of the interactions.

In conclusion, we have considered the functionality of a Brownian ratchet and investigate the role of hydrodynamic interactions on the efficiency of this system. To take into account the interactions with walls of the channel, we proceeded with an approximate scheme for the mobility tensor of a colloidal particle moving near boundaries. We discussed the limitations and validity of this approximation. As there is no exact solution for the mobility of a particle inside channel, to achieve more accurate results one can perform a simulation that includes coupled equations of motion for colloidal particles and also the fluid particles. Although the results of such intense studies will help to obtain more accurate results, we do not expect to see a large qualitative deviation with the results that we have obtained here.

## ACKNOWLEDGMENT

We wish to acknowledge useful discussions with M. Maleki.

[1] M. von Smoluchowski, Phys. Z. **XIII**, 1069 (1912).
[2] R. Feynman, *Lectures on Physics* (Addison-Wesley, Longman, 1997).
[3] P. Eshuis, K. van der Weele, D. Lohse, and D. van der Meer, Phys. Rev. Lett. **104**, 248001 (2010).
[4] F. Julicher, A. Ajdari, and J. Prost, Rev. Mod. Phys. **69**, 1269 (1997).
[5] N. S. Lin, T. W. Heitmann, K. Yu, B. L. T. Plourde, and V. R. Misko, Phys. Rev. B **84**, 144511 (2011).
[6] C. Kettner, P. Reimann, P. Hanggi, and F. R. Muller, Phys. Rev. E **61**, 312 (2000).
[7] P. Reimann, Phys. Rep. **361**, 57 (2002).
[8] D. Reguera, A. Luque, P. S. Burada, G. Schmid, J. M. Rubí, and P. Hanggi, Phys. Rev. Lett. **108**, 020604 (2012).
[9] S. Martens, G. Schmid, A. V. Straube, L. Schimansky-Geier, and P. Hanggi, Eur. Phys. J. Spec. Top. **222**, 2453 (2013).
[10] S. Martens, I. M. Sokolov, and L. Schimansky-Geier, J. Chem. Phys. **136**, 111102 (2012).
[11] P. Hänggi and F. Marchesoni, Rev. Mod. Phys. **81**, 387 (2009).
[12] A. Grimm and H. Stark, Soft Mater **7**, 3219 (2011).

[13] A. Pralle, E.-L. Florin, E. H. K. Stelzer, and J. K. H. Hörber, Appl. Phys. A **66**, S71 (1998).
[14] E. R. Dufresne, T. M. Squires, M. P. Brenner, and D. G. Grier, Phys. Rev. Lett. **85**, 3317 (2000).
[15] S. H. Rad and A. Najafi, Phys. Rev. E **82**, 036305 (2010).
[16] J. P. Hernandez-Ortiz, C. G. Stoltz, and M. D. Graham, Phys. Rev. Lett. **95**, 204501 (2005).
[17] A. Najafi, S. S. H. Raad, and R. Yousefi, Phys. Rev. E **88**, 045001 (2013).
[18] S. Martens, A. V. Straube, G. Schmid, L. Schimansky-Geier, and P. Hanggi, Phys. Rev. Lett. **110**, 010601 (2013).
[19] P. M. Chaikin and T. C. Lubensky, *Principles of Condensed Matter Physics* (Cambridge University Press, Cambridge, England, 1995).
[20] J. W. Swan and J. F. Brady, Phys. Fluids **19**, 113306 (2007).
[21] N. Liron and S. Mochon, J. Eng. Math. **10**, 287 (1976).
[22] J. Happel and H. Brenner, *Low Reynolds Number Hydrodynamics* (Noordhoff, Leyden, 1973).
[23] B. Lin, J. Yu, and S. A. Rice, Phys. Rev. E **62**, 3909 (2000).
[24] D. L. Ermak and J. MacCammon, J. Chem. Phys. **69**, 1352 (1978).